

Tetragonal silver films on V(100): Experimental and *ab initio* studies

Marko Kralj,* Petar Pervan, and Milorad Milun
Institute of Physics, P.O. Box 304, Zagreb HR-10000, Croatia

Predrag Lazić, Željko Crljen, and Radovan Brako
Rudjer Bošković Institute, P.O. Box 180, Zagreb HR-10000, Croatia

Jörg Schneider, Axel Rosenhahn, and Klaus Wandelt
Institute for Physical and Theoretical Chemistry, Wegelerstrasse 12, Bonn D-53115, Germany
 (Received 20 May 2003; revised manuscript received 18 July 2003; published 6 November 2003)

The growth and structure of ultrathin silver films (1–5 monolayers thick) deposited on a reconstructed V(100)-(5×1) surface have been studied by means of scanning tunneling microscopy (STM), Auger electron spectroscopy (AES), and angle-resolved photoemission spectroscopy (ARPES). To model the structure of the system we have also performed density functional (DFT) calculations. It has been established that due to the annealing of deposited silver uniform films are formed and that the vanadium reconstruction is completely removed. As found from STM measurements and supported by *ab initio* calculations in the in-plane direction silver follows the structure of the V(100)-(1×1) lattice and is tetragonally distorted in the direction perpendicular to the surface. In addition, *ab initio* results predicted the adsorption energies of individual silver layers and the work function of Ag/V(100), both in accordance with experiments.

DOI: 10.1103/PhysRevB.68.195402

PACS number(s): 68.55.Jk, 68.35.Fx, 68.37.Ef, 68.65.–k

I. INTRODUCTION

Ultrathin metal films (MF's) on metal substrates (MS's) are a subject of continuous extensive investigations. The points that are of fundamental interest include new structural and electronic properties. Pseudomorphic film growth may lead to a different structure with respect to the bulk form and to novel electronic and magnetic properties. Formation of discrete electronic states, so-called quantum well states (QWS's), is one of the intriguing electronic phenomena observed in ultrathin films.^{1–3} In that respect ultrathin silver films on various substrates have been studied. Silver growth on transition metal surfaces Fe(100),⁴ V(100),⁵ and W(110) (Ref. 6) shows many of the desired properties required for the formation of QWS's. Silver grows layer-by-layer in the limit of ultrathin films on all three surfaces. In the case of Fe(100) this growth can extend to film thicknesses well above 100 monolayers (ML).⁴ The electronic structure of the substrate surfaces provides a hybridization gap that induces localization within the silver overlayer film for the electrons of *s-p* and *d* symmetry. Although simple phase models have shown a significant success in understanding the formation of quantum well states in these systems, it is obvious that only *ab initio* calculations can provide a full insight into the complex nature of the interaction of electronic states in the overlayer film and substrate.

Recent studies of Ag/V(100) have been dominantly focussed on the electronic properties.^{1,5,7–11} The available structural data from previous studies show that at the substrate temperature of around 300 K silver can grow on V(100) pseudomorphically in a layer-by-layer fashion up to 10 monolayers (ML).^{12,13} Also, it was only assumed that the silver film has a tetragonal structure, based on a simple hard-sphere picture.⁵ The tetragonal structure, however, was never confirmed by measurements [*I-V* low energy electron diffraction (LEED) or scanning tunneling microscopy (STM),

for example] or calculations, and good pseudomorphic growth was qualitatively attributed to the relatively small lattice mismatch of 4.5% between the fcc Ag(100) and bcc V(100) planes, and to the favorable small surface free energy for silver of 1.3 J m^{-2} , compared to the relatively large value for vanadium of 3 J m^{-2} .

Recently, a first principle calculation of electronic properties of Ag on V(100) was reported.¹⁴ In that work the structure of the underlying vanadium as well as the overlayer silver film was constructed from the vanadium bulk values and a hard sphere model, respectively. Some of the results differ substantially from the published experimental data, e.g., the work functions are 0.5–1.5 eV larger than the experimental values.¹⁵

In this work we present results of a combined experimental and computational investigation of the Ag/V(100) structure in the thickness range of 1–5 ML. STM, Auger electron spectroscopy (AES), angle-resolved photoelectron spectroscopy (ARPES), and LEED were used to characterize ultrathin silver layers. Compared to previous Ag/V(100) studies, where silver was deposited on an unreconstructed V(100) substrate, we show here that we can prepare the Ag/V(100) system by depositing silver on the reconstructed V(100)-(5×1) surface, which is experimentally much easier. This is due to the fact that the vanadium reconstruction is completely lifted upon silver deposition and thermal treatment, as confirmed with AES, LEED, STM, and ARPES measurements. STM results prove the tetragonal structure of the silver overlayer in full agreement with our *ab initio*, self-consistent calculations. The calculations provide valuable information on the relaxation effects in the silver film and in the first layers of the underlying vanadium substrate. From the calculation we also obtain values of the adsorption energies of individual silver layers and the realistic values of V(100) and Ag/V(100) work functions.

II. EXPERIMENTAL AND COMPUTATIONAL DETAILS

The experiments were carried out in three different ultra-high vacuum systems. While the chambers in Zagreb and Bonn were equipped with the same type of a home-built STM,¹⁶ in the first one LEED, AES, and ARPES (VSW HA 100 analyzer), and in the second one AES (cylindrical mirror analyzer), were additionally available. Parts of the photoemission experiment were carried out at Elettra synchrotron at the 3.2 R VUV beam line¹⁷ in the photon energy range 19–95 eV. The energy and angular resolution of the VSW HA 50 analyzer was 30 meV and $\pm 0.5^\circ$, respectively. In the UHV chamber at Elettra a quartz microbalance was also available to estimate the quantity of the deposited silver. The base pressure in each system was in the 10^{-11} mbar region. Throughout all experiments one and the same V(100) single crystal was used. The (5×1) reconstructed V(100) surface that served as a substrate for silver growth was prepared according to a procedure described elsewhere.¹⁸ Silver was evaporated by the resistive heating of a tungsten basket containing a silver droplet. The deposition rate was adjusted to be 0.2–1 ML/min.

The *ab initio* calculations of the electronic properties of the Ag/V(100) structures were performed in the density-functional theory (DFT) approach, using the DACAPO computer code.¹⁹ We have used the provided ultrasoft pseudopotentials for the Perdew-Wang exchange-correlation functional PW91 and the generalized gradient approximation (GGA).²⁰ The crystal structures were modeled by the slab geometry where the vanadium substrate consists of seven layers on top of which we add silver layers (1–5 ML). We have also checked our calculations by modeling the vanadium substrate by eight and ten layers and found virtually no changes in the results. We applied periodic boundary conditions in the directions along the surface plane (coordinates x , y). The starting point in the calculations was the clean and unreconstructed V(100) surface, although the substrate surface in the experiments was the (5×1) reconstructed vanadium surface. This is fully justified by the fact that silver films lift the reconstruction after annealing at elevated temperatures, as is described later in the text.

The bottom three layers of vanadium were kept fixed at the bulk separation, while the other vanadium and silver layers were allowed to relax in the direction of the surface normal (coordinate z). In the z direction the slabs were separated by a layer of vacuum of around 15 Å. This is sufficiently thick so that the periodic repetition, which is built in the computational method does not affect the final result of the calculation. We used a mesh of 12×12 k points in the x - y plane, an energy cutoff of 440 eV, and a pseudothermal smearing of the electron occupation corresponding to a temperature of $T = 0.2$ eV.

We also calculated the work functions. In calculation of the work function the DACAPO program provides a special feature that includes the dipole correction at the surface, as discussed by Bengtsson,²¹ which is essential in order to obtain accurate values of the work function.

The calculations were done assuming a nonmagnetic electronic wave function. However, before doing so, we per-

formed calculations for a clean V(100) surface and for one monolayer of Ag on V(100) allowing for the spin polarization. Although the initial condition in these calculations was a large magnetic moment on the first few layers, the electronic wave function quickly converged to a nonmagnetic solution.

III. RESULTS

A. Preparation of ordered silver layers

In this study the (5×1) reconstructed vanadium (100) surface was used as a substrate to grow the silver films mainly because the V(100)- (5×1) surface preparation is rather simple, particularly so when compared to the preparation of the clean and ordered unreconstructed V(100) surface. Previous investigations have shown that the deposition and annealing of already ≈ 0.5 ML of silver on an oxygen-precovered V(100) produces an oxygen-free interface and film.²² It has also been shown that a clean V(100) surface endures, at best, about 800 K annealing temperature without segregating oxygen and carbon to the surface. Such a modest temperature is not ideal to produce very large, flat, and defect free V(100) terraces. In the case of the (5×1) reconstructed V(100) surface, during the last stages of surface preparation the sample is annealed to significantly higher temperatures (typically 1200 K) which leads to segregation of (mainly) oxygen and the formation of large and well ordered (5×1) reconstructed terraces.¹⁸ Subsequent deposition of silver and annealing at 600–900 K results in the complete removal of oxygen from the silver-vanadium interface and a complete transition of the (5×1) reconstruction to the (1×1) structure of the clean V(100) surface.

The film preparation process can be divided into three steps: (a) the V(100)- (5×1) substrate preparation, (b) the silver deposition while the substrate is kept at room temperature, and (c) annealing at a selected temperature. Each of these steps may be followed in subsequent STM and AES measurements, as shown in Fig. 1. In the large-scale STM image shown in Fig. 1(a), a footprint of the (5×1) vanadium reconstruction is seen as bright stripes equidistantly separated by thin dark lines. In fact, there are two domains rotated by 90° . The corresponding AES spectrum is shown in Fig. 1(d): it clearly indicates the presence of oxygen on the vanadium surface. We have deposited approximately 1.5 ML of Ag on the surface at room temperature. The result is seen in the STM image in Fig. 1(b) and the corresponding AES spectrum is shown in Fig. 1(e). The result of the silver deposition is the formation of 3D silver clusters with the presence of oxygen on the vanadium surface [Fig. 1(e)]. This is an indication that, at this stage, the vanadium surface remains reconstructed.

The next step is the annealing of the sample up to 750 K for 1 min. The AES spectrum [Fig. 1(f)] shows a significant increase of the silver to vanadium intensity ratio from 0.57, prior to annealing, to 0.85 after annealing. At the same time, the oxygen and carbon Auger signals (the latter not shown in the spectra) diminish, indicating that these elements diffuse out of the near surface region. The STM image [Fig. 1(c)] reveals the formation of ordered and flat 2D silver terraces.

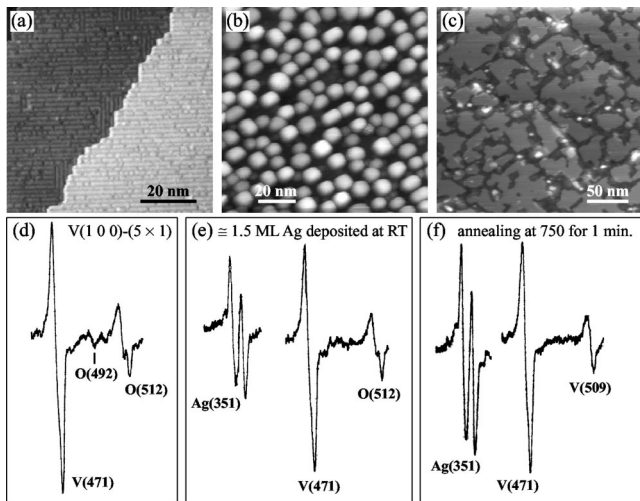


FIG. 1. Steps of preparation of uniform silver films used in this work. (a) STM image of the V(100)-(5 \times 1) substrate ($I_T = 1.5$ nA, $U_B = 0.54$ V). (b) STM image of ≈ 1.5 ML of Ag deposited onto the V(100)-(5 \times 1) surface at RT ($I_T = 0.1$ nA, $U_B = 0.84$ V). (c) STM image of the same surface as in (b) after a flash to 750 K ($I_T = 0.1$ nA, $U_B = -0.056$ V). (d)–(f) AES spectra corresponding to the surfaces shown in (a)–(c), respectively. In panels (d)–(f) the x axis presents the kinetic energy and the y axis the first derivative of the Auger electron intensity.

In the case of silver nominal coverages higher than 2 ML the annealing induces a Stranski-Krastanov growth mode with a 2 ML thick silver layer as a substrate for the clusters of the excess silver. The excess silver can be desorbed by annealing the sample at the temperature of the silver desorption onset (900 K).^{12,13} The result is a perfectly ordered 2 ML thick layer that later may serve as a substrate for layer-by-layer deposition of thicker silver films (at or somewhat below the room temperature). Due to a difference of 50 K in the desorption temperatures of the first and the second silver film from the V(100) surface it is possible to desorb the second layer and obtain extremely well ordered single silver layer.

Figure 2 shows a set of normal emission ultraviolet photoemission spectra taken during different stages of the silver film preparation, as described above. The bottom spectrum is taken from the well annealed V(100)-(5 \times 1) substrate. In the next spectrum one sees that the deposition of silver at room temperature strongly modifies the region previously dominated by the O 2*sp* valence band and reduces the intensity at the Fermi level. However, within the *s-p* silver band region no sharp peaks are formed, and within the *d*-band region we find two broad peaks located around binding energy of 4.9 and 6.1 eV. For this particular experiment the nominal silver coverage was about 4 ML. The film was first flashed to 800 K and afterwards to 900 K. In the photoemission spectra new features occurred in both the *s-p* and *d* regions. These peaks correspond to the emission from QW states. Previous studies have shown that their binding energy is thickness dependent and that they can be reliably used as reference points for the silver thickness calibration.⁵ The photoemission spectra in Fig. 2 are characteristic for the 2 and 1 ML thick silver films, respectively. The sharp and in-

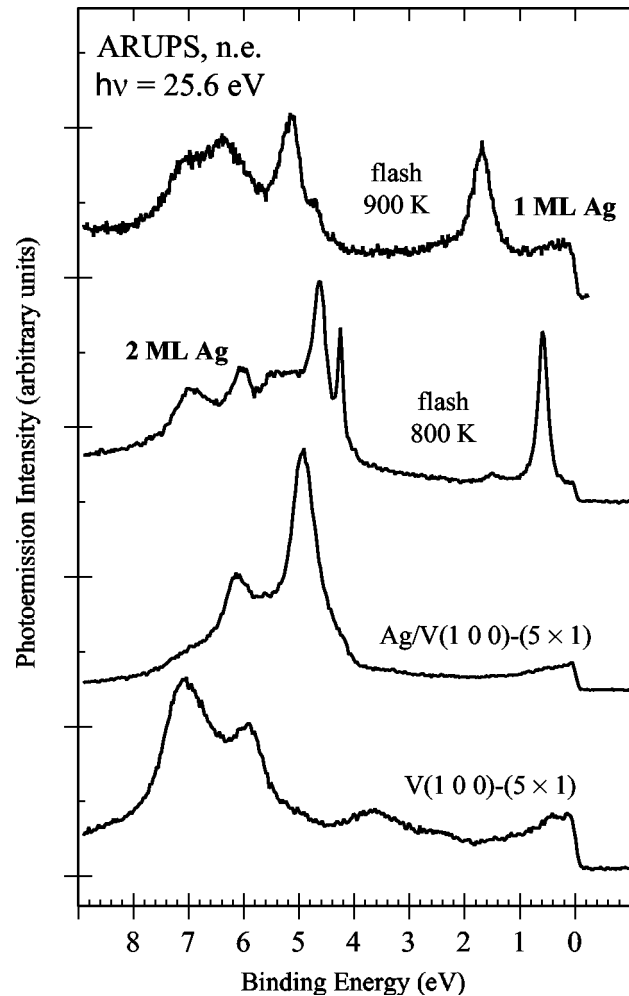


FIG. 2. Normal emission ultraviolet photoemission spectra characterizing the silver film formation on the V(100)-(5 \times 1) substrate. The intensities are normalized to the photon flux. From the bottom to the top: the bare substrate, ≈ 4 ML of Ag deposited at RT, flashed to 800 K, flashed to 900 K.

tense QW peaks indicate a high degree of order of the silver films. This is also confirmed by LEED measurements. All samples show sharp (1 \times 1) diffraction spots on low background, the same pattern as the clean and well ordered V(100) surface. Thicker films, up to 5 ML, were prepared by subsequent silver deposition on a well ordered 2 ML film. They are stable up to ≈ 350 K, while at higher temperatures the Stranski-Krastanov growth mode prevails, as described above. It starts with the formation of multilayers as evidenced from the QW state photoemission peaks, especially when variable photon energy is used to optimize the QW peak photoionization cross section (see Fig. 10 in Ref. 8).

B. STM measurements

In the regime where the initially deposited silver quantity was less than nominally 1 Ag ML we could study the height of individual silver monolayer islands. The experiments have shown that STM imaging of silver islands is a quite delicate procedure. During the scan an island is sometimes shifted in

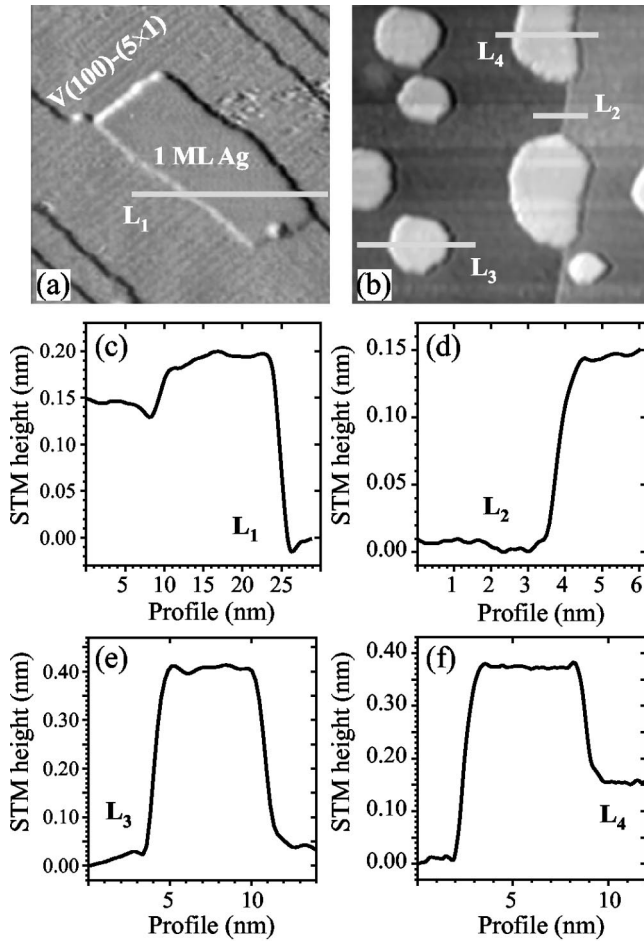


FIG. 3. (a) STM image showing 1 ML thick silver island formed on the V(100)-(5 \times 1) substrate (image size 46 \times 46 nm², $I_T=1.2$ nA, $U_B=0.45$ V). (b) STM image showing 2 ML thick silver islands formed on the V(100)-(5 \times 1) substrate (image size 34 \times 34 nm², $I_T=0.5$ nA, $U_B=0.4$ V). (c)–(f) Profile scans taken across the (a) and (b) images indicated by thick gray lines.

position or damaged in such a way that holes are created along with the appearance of new terraces. For the submonolayer silver coverage no preferential nucleation regions are found, i.e., some islands are aligned along the vanadium step edges and some are formed in the middle of terraces [see Figs. 3(a) and 3(b)]. Figure 3(a) illustrates the case where a silver island is formed at the vanadium step edge. In this STM image the vanadium (5 \times 1) reconstruction is clearly visible [for comparison check Fig. 1(a)]. The profile line scan L_1 [see Fig. 3(c)] clearly shows the difference in height between the vanadium step and the silver monolayer. When going from right to left along L_1 the STM tip goes across a vanadium terrace upon which the Ag island is adsorbed, which is used as zero in STM height measurements, then crosses the Ag island and descends to the upper vanadium terrace. From a large number of similar independent measurements on many islands we obtained both the value for a silver monolayer height of 1.8 ± 0.2 Å and the value of 1.5 ± 0.1 Å for the vanadium single-atom step height.

In a similar way and by using the procedures described above for the formation of thicker films, we could study

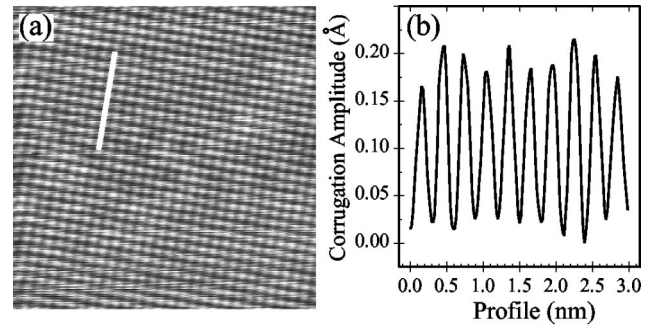


FIG. 4. (a) Atomically resolved STM image of the 2 ML Ag/V(100) surface. Image size 7.8 \times 7.8 nm², $I_T=19$ nA, $U_B=0.025$ V. (b) Profile scan along the white line indicated in the STM image.

isolated islands of up to 5 ML. Figure 3(b) shows an STM image where 2 ML thick silver islands dominate. Three profile scans [shown in Figs. 3(d)–3(f)] were taken at different locations in the image in order to determine the height of the second silver layer. Within the resolution of our STM measurements we find that the second silver layer has an STM derived height of 2.0 ± 0.1 Å. This value is also found for all additional monolayers at all studied coverages.

Figure 4(a) shows a Fourier filtered atomically resolved image of the 2 ML thick silver film. Clearly, the (1 \times 1) quadratic structure imaged in the STM experiment is consistent with the LEED measurements. A profile scan taken along the white line is shown in Fig. 4(b). Note that the typical atomic STM corrugation amplitude is 0.2 Å. From the drift-corrected images in a thickness range 1–5 ML we have calculated angular correlation images and obtain an in-plane Ag-Ag interatomic distance of 3.0 ± 0.1 Å, which is, within the accuracy of our STM experiment, the value of the lattice parameter of the unreconstructed vanadium (100) surface.

C. *Ab initio* calculations

In order to find the structural parameters of Ag and V, we first calculated the properties of the bulk metals. The optimal lattice constant of 3.00 Å for the vanadium bcc cell was obtained, which gives the energy minimum in the calculation of the vanadium bulk for the used pseudopotential. This value differs slightly (1%) from the real value of the vanadium bcc cell (3.03 Å).²³ This approach, however, ensures that no spurious bulk stresses appear. For the fcc silver the lattice constant was found to be 4.14 Å, 1.5% larger than the real value of 4.09 Å.²³ Thus the mismatch of the lattice constant of the pseudomorphically grown silver adlayers is only 2.5% in our calculations, instead of 4.5% in the experiment. Although it is commonly accepted that adsorbed metal atoms on metal surfaces, in cases when there is a relatively small lattice mismatch, occupy adsorption sites of highest coordination, we have nevertheless explored the adsorption geometry of the Ag/V(100) system. In order to evaluate the adsorption energy of a silver atom in different positions we have commensurably added a silver monolayer on the V(100)-(1 \times 1) surface in three possible variants, where sil-

TABLE I. Calculated structural parameters of the clean (1×1) vanadium surface and of pseudomorphically grown silver films. Given are the step heights for each additional ML of silver (in Å), the interlayer distance (in Å), the work function (in eV), and the adsorption energy of silver, i.e., the energy gain compared to the previous adlayer and an isolated silver atom (in eV). A vanadium slab consisting of seven layers was used in the calculations, and the bottom three layers were kept at the fixed separation of 1.50 Å.

	Clean V	1 ML Ag	2 ML Ag	3 ML Ag	4 ML Ag	5 ML Ag
Step height		1.95	1.99	1.96	1.99	1.95
Ag ₄ -Ag ₅						1.94
Ag ₃ -Ag ₄					1.93	2.00
Ag ₂ -Ag ₃				1.95	1.99	1.98
Ag ₁ -Ag ₂			1.95	2.00	1.98	1.98
V ₁ -Ag ₁		1.86	1.89	1.88	1.85	1.86
V ₁ -V ₂	1.32	1.39	1.41	1.38	1.42	1.38
V ₂ -V ₃	1.48	1.46	1.47	1.46	1.48	1.49
V ₃ -V ₄	1.54	1.53	1.54	1.52	1.50	1.51
V ₄ -V ₅	1.46	1.51	1.47	1.52	1.54	1.48
V ₅ -V ₆ , etc.	1.50	1.50	1.50	1.50	1.50	1.50
Work function	3.93	4.34	4.34	4.35	4.26	4.32
Adsorption energy		3.02	2.62	2.54	2.59	2.58

ver atoms occupied on-top, bridge or fourfold hollow positions, respectively. Our results clearly show that, as expected, the energetically most favorable position for the silver atom on a V(100) surface is the fourfold hollow site (silver adsorption energy of 3.02 eV/atom), in contrast to the energetically unfavorable bridge (2.59 eV/atom) or on-top (2.33 eV/atom) positions.

Further we have calculated structural parameters in the system for different silver thicknesses. The first silver layer was added with all atoms in the hollow sites, which corresponds to a pseudomorphical growth with the fcc cell rotated by 45° . The tetragonal distortion of the pseudomorphic Ag adlayers is caused by the fact that its lattice constant in the x - y plane is 2.5% larger than the preferred Ag bulk value, and as a consequence the lattice constant in the z direction shrinks. By doing calculations for bulk silver with tetragonal distortion, we found that the optimum interlayer distance is 5% smaller and that the energy per atom is only 4 meV larger than that of the undistorted fcc silver. Even if the smaller mismatch of the bulk lattice constants in the calculations leads to an underestimate of the energy difference, it is clear that the difference is small and that the tetragonally distorted silver layers are quite stable.

In Table I we show the calculated interlayer separations of the vanadium surface and up to five silver adlayers. The bottom three layers of vanadium were kept fixed at the bulk separation of 1.5 Å, while the top four layers, as well as the silver adlayers, were allowed to relax. In the case of uncovered V surface, the separation between the first and the second layer is reduced by around 13% with the respect to the bulk value. This has been observed already both experimentally and obtained in calculations (Ref. 24, and references therein). The separation between deeper layers departs from the bulk value in either direction by up to around 2%. With

silver adlayers, the distance between the first and the second vanadium layer is reduced by 5–8%, considerably less than on the clean vanadium surface. The oscillatory relaxation pattern between deeper vanadium layers persists, and in fact might propagate even deeper if a thicker vanadium slab was used in the calculations. However, the associated relaxation energy is too small to affect the overall picture.

Also given in Table I are the calculated height differences between successive silver layers which agree well with the values determined by STM. However, one should bear in mind that the calculated values are, in fact, the differences of positions of the atom nuclei, while STM probes the electronic density profile. Furthermore, the height of the silver monolayer is calculated with respect to the relaxed vanadium (1×1) surface, which is the situation very close to the experimental one when the Ag layer covers the entire surface area. This may differ somewhat in the case of small silver islands coexisting with free (5×1) reconstructed vanadium surface patches, which may on average be less contracted inwards. The obtained structural results are also shown in Fig. 5 for an example of an uncovered V(100) surface, and with 2 ML of silver on V(100). In the figure we have also indicated the z coordinates for each atomic layer for the clearer comparison of the two structures. The z coordinates are given with respect to the relaxed bare V(100) surface and its topmost layer in the position of the origin.

We also determined the energies of adsorption of Ag atoms into the various adlayers. For comparison, the value of the bulk cohesion energy of silver is 2.57 eV/atom in our calculations. The absolute values may be affected by the method of the calculation, especially the energy of an isolated atom, but the energy differences are much less susceptible. Very prominent is the large value of the energy of

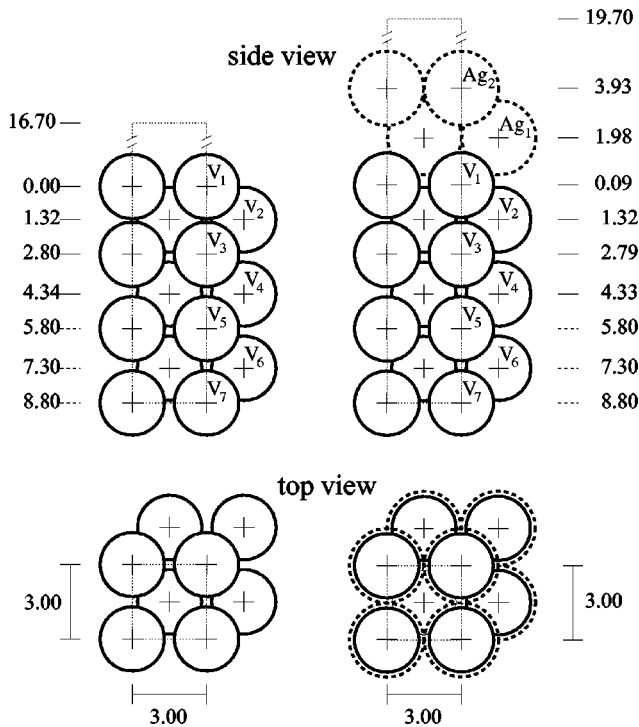


FIG. 5. The side and top view of the unit cells (dotted lines) used in the calculations of a clean V(100) surface (left), and of 2 ML Ag on V(100) (right). The dimensions of the unit cells and the positions of the atoms (circles) after relaxation are given in Å. The z coordinate is chosen so that the first layer of the relaxed bare V(100) surface is at zero. The bottom three vanadium layers (V_5 – V_7) are kept fixed at bulk separation.

adsorption into the first layer of more than 3 eV. The minimum of the adsorption energy of 2.54 eV/atom occurs for the third monolayer (3 ML film). The value is smaller than for both the second and the fourth layer, which means that it is energetically favorable for 3 ML films to disproportionate into 2 and 4 ML, if the energy cost of the step edge which must be created is not too high. In Table I we also show the results for the work function of the clean and silver covered V(100) surfaces. The values of 3.93 eV for a clean surface and around 4.3 eV for silver covered surfaces are in excellent agreement with experiment.^{12,15}

IV. DISCUSSION

There are two issues that we address here. The first one is that upon deposition of silver and subsequent annealing of the sample, the vanadium (5×1) reconstruction beneath the silver overlayer can be completely removed and the structure of a clean and well ordered V(100) restored. Second, we discuss experimental and theoretical evidence for the tetragonal structure of the silver overlayer films.

A. Formation of the Ag/V(100) interface; removal of the (5×1) reconstruction

Valla *et al.*²² studied the effects of silver deposition on the oxygen precovered clean and ordered V(100). At room temperature and below they found the effects of disordering of

the silver film. Moreover, they concluded that not only oxygen disorders the silver film, but most probably it occupies the Ag/V interface sites which is driven by the high affinity towards atomic oxygen of both vanadium and silver. Investigating the effects of annealing they found that up to 570 K no significant changes are present. At higher annealing temperatures the ordered structure of the silver layer is gradually restored and finally after annealing at 710 K no oxygen-derived emission is found in the ARPES, XPS, or AES spectra anymore and the order in the silver film is completely restored, which was also confirmed by LEED.

The removal of oxygen from the vanadium surface upon adsorption and annealing of silver deposits is the desired scenario for the formation of well defined ultrathin silver films on V(100). However, such favorable interaction of deposited metal films with oxygen on the vanadium surface appears to be an exception rather than a rule. Recently, Konvicka *et al.*²⁵ studied the Pd growth on the V(100)-(5×1) surface. Based on STM and AES results they concluded that for the submonolayer coverage of 0.15 ML and room temperature single Pd atoms are trapped (stabilized) in the free fourfold co-ordinated hollow sites, i.e., sites unoccupied by oxygen or carbon atoms. This is explained with stronger affinity, i.e., bonding energies, of palladium to vanadium in the clean fourfold hollow sites compared to other available sites on the surface. Further, when annealed at 470 K, Pd forms small islands while the O and C atoms leave the Pd-V interface forming a more dense adlayer around the Pd islands.²⁵ For higher coverages the Pd growth proceeds only on areas free of oxygen which limits the size of Pd islands and leaves parts of the surface covered with the dense (1×1) oxygen layer which is acting as antisurfactant for the growth of the Pd islands.²⁵

Obviously, in both systems [Pd/V(100)-(5×1) and Ag/O/V(100)], the annealing temperature plays a very important role as is the case for the system Ag/V(100)-(5×1) studied here. At room temperature oxygen atoms that occupy (preferentially) fourfold vanadium sites are not mobile enough to diffuse across or out from the surface. For oxygen, the diffusion from the surface into the bulk and vice versa, is efficient at annealing temperatures of ≈ 700 K and higher and as a result many fourfold sites are temporarily free. If there is an Ag atom in the vicinity such a site is immediately occupied by it. Our calculations suggest that there is a net energy gain per Ag atom of almost half eV when an atom leaves the Ag bulk (e.g., an Ag cluster) and sticks to a fourfold vanadium site. This energy gain seems to be substantially larger than the cost of pushing an oxygen atom back into the bulk. In such a way the formation of large silver islands takes place. The uncovered V(100)-(5×1) patches remain in their original structure. There is no compression of the oxygen (and carbon) atoms as is observed in the case of the Pd/V(100)-(5×1) system.²⁵ Thermal desorption measurements show that there is no desorption of O₂ and O species during annealing at these temperatures. Therefore, we conclude that oxygen atoms diffuse into the vanadium bulk.

The differences in the properties of the Ag/V(100)-(5×1) and Pd/V(100)-(5×1) can be qualitatively explained if one takes simple geometry and energy considerations into

account. First of all, the lattice mismatch between the vanadium bcc(100) lattice is much smaller for silver fcc(100) (4.5%) than for palladium fcc(100) (9%). Another point of difference is the surface free energy balance which again favors the ordered silver film. The surface free energy is $\approx 3 \text{ J/m}^2$ for vanadium, $\approx 1.9 \text{ J/m}^2$ for palladium, and $\approx 1.3 \text{ J/m}^2$ for silver. Clearly, a silver layer minimizes the surface free energy more efficient than palladium. This is in agreement with thermal desorption measurements of Valla and Milun¹² which show that the stability of the first silver layer is very high reflecting the strong silver-vanadium bonding which in this case is much stronger than the silver-silver bonding. This is also found in the aforementioned calculated large energy of the adsorption of silver atoms into the first V(100)-(1×1) layer, which indicates the tendency of the silver to remove the (5×1) reconstruction of the vanadium surface.

B. Tetragonal silver

The ordered bcc, bct, or hcp growth of otherwise fcc materials has already been observed, for instance, for copper^{26,27} and palladium films²⁷ on various substrates. For copper a nonequilibrium thin crystal structure is stable due to the only slightly larger volume energies of the equilibrium fcc structure. Pd epitaxially follows the substrate in the Pd/W(100) system because the atomic radii of W and Pd are almost identical. The structure of very thick films is determined by the difference in the volume energy and always tends towards the bulk structure. In the situation where a nonequilibrium crystal structure provides much better fit to the substrate lattice than any other orientation of the bulk crystal structure, the smaller stress can make a nonequilibrium structure energetically more favorable over a large thickness range.

For ultrathin silver films on V(100) we have presented here clear experimental and *ab initio* results which show that 1–5 ML thick silver films on V(100) have a tetragonal structure. Experimental evidence comes from the STM height measurements. We are, however, aware that one should be particularly cautious, since STM is actually sensitive to changes in the charge density and not merely the topography.

Nevertheless, a substantial difference between the vanadium and silver terraces heights of 0.3–0.5 Å and the measured height between silver layers of $2.0 \pm 0.1 \text{ Å}$ points to tetragonal distortion of the silver film in the direction perpendicular to the surface, whereas at the same time the in-plane lattice parameter perfectly matches the lattice parameter of the underlying vanadium substrate.

From *ab initio* calculations we have obtained structural parameters of the Ag/V(100) system. The values of interlayer separations are in a very good agreement with the STM results establishing a clear picture of tetragonally distorted sil-

ver films. Moreover, calculations enabled us to additionally probe the fine structural details which were not accessible in the experiment. This concerns detailed relaxations of interlayer spacings of the first few vanadium layers as well as of silver adlayers. We have shown that upon the deposition of silver a stable tetragonal structure induces changes between the vanadium interlayer spacings. This is especially pronounced between the first and the second vanadium layer where the tendency of silver to decrease the stress of the vanadium minimizes the overall energy of the system. Therefore we believe that the proper structural information is very important for calculations concerning the silver-vanadium interface.

V. CONCLUSIONS

In conclusion, we have investigated the structure of 1–5 ML thick Ag films on the V(100) surface. The substrate surface in the experiment was the (5×1) reconstructed V(100) surface. This surface is a favorable substrate for the formation of ordered ultrathin silver films since it is relatively easy to prepare a well-ordered V(100)-(5×1) surface. We followed the formation of ordered silver layers by means of AES, STM, ARPES, and LEED and showed that upon deposition and annealing the silver lifts the reconstruction of the underlying vanadium and oxygen atoms are displaced from the surface and diffuse into the bulk. In this way uniform layers of 1 or 2 ML thickness are formed and serve as a substrate for the deposition of thicker silver layers. The removal of the vanadium reconstruction is explained by a very large adsorption energy of silver atoms into the fourfold sites on the vanadium surface ($\approx 3 \text{ eV/atom}$) which minimizes the energy of the system.

The tetragonal structure of ordered silver layers was probed with STM. The in-plane lattice parameter of silver matches the in-plane parameter of the vanadium, while, on the other hand, silver is tetragonally distorted in a direction perpendicular to the surface. The STM heights of the silver terraces and the calculated values are in excellent agreement. The calculations provide additional valuable detailed structural information regarding the relaxation of the first few vanadium interlayer separations, the workfunction and the adsorption energy for 1–5 silver layers.

ACKNOWLEDGMENTS

The financial supports of the Ministry of Science and Technology of the Republic of Croatia (IF group—Project No. 0035016; IRB group—Project No. 0098001) and the bilateral Croatian-German project (“Preparation and Characterization of Metallic Nano-Structures,” Project No. KRO-013-97) are gratefully acknowledged.

*Email address: mkralj@ifs.hr

¹M. Milun, P. Pervan, and D. P. Woodruff, Rep. Prog. Phys. **65**, 99 (2002).

²T.-C. Chiang, Surf. Sci. Rep. **39**, 181 (2000).

³F. J. Himpsel, J. E. Ortega, G. J. Mankey, and R. F. Willis, Adv.

Phys. **47**, 511 (1998).

⁴J. J. Paggel, T. Miller, and T.-C. Chiang, Science **283**, 1709 (1999).

⁵T. Valla, P. Pervan, M. Milun, A. B. Hayden, and D. P. Woodruff, Phys. Rev. B **54**, 11 786 (1996).

- ⁶A. M. Shikin, O. Rader, G. V. Prudnikova, V. K. Adamchuk, and W. Gudat, *Phys. Rev. B* **65**, 075403 (2002).
- ⁷P. Pervan, M. Milun, and D. P. Woodruff, *Phys. Rev. Lett.* **81**, 4995 (1998).
- ⁸M. Milun, P. Pervan, B. Gumhalter, and D. P. Woodruff, *Phys. Rev. B* **59**, 5170 (1999).
- ⁹D. P. Woodruff, M. Milun, and P. Pervan, *J. Phys.: Condens. Matter* **11**, L105 (1999).
- ¹⁰T. Valla, M. Kralj, A. Šiber, M. Milun, P. Pervan, P. D. Johnson, and D. P. Woodruff, *J. Phys.: Condens. Matter* **12**, L477 (2000).
- ¹¹M. Kralj, A. Šiber, P. Pervan, M. Milun, T. Valla, P. D. Johnson, and D. P. Woodruff, *Phys. Rev. B* **64**, 085411 (2002).
- ¹²T. Valla and M. Milun, *Surf. Sci.* **315**, 81 (1994).
- ¹³T. Valla, P. Pervan, and M. Milun, *Vacuum* **46**, 1223 (1995).
- ¹⁴A. Ernst, J. Henk, M. Lüders, Z. Szotek, and W. M. Temmerman, *Phys. Rev. B* **66**, 165435 (2002).
- ¹⁵T. Valla, P. Pervan, M. Milun, and K. Wandelt, *Surf. Sci.* **347**, 51 (1997).
- ¹⁶M. Wilms, M. Schmidt, G. Bermes, and K. Wandelt, *Rev. Sci. Instrum.* **69**, 2696 (1998).
- ¹⁷For the details on the beam line see URL <http://www.elettra.trieste.it/experiments/beamlines/vuv/index.html>
- ¹⁸M. Kralj, P. Pervan, M. Milun, K. Wandelt, D. Mandrino, and M. Jenko, *Surf. Sci.* **526**, 166 (2003).
- ¹⁹B. Hammer, L. B. Hansen, and J. K. Nørskov, *Phys. Rev. B* **59**, 7413 (1999); URL <http://www.fysik.dtu.dk/CAMP/dacapo.html>
- ²⁰J. P. Perdew, J. A. Chevary, S. H. Vosko, K. A. Jackson, M. R. Pederson, D. J. Singh, and C. Fiolhais, *Phys. Rev. B* **46**, 6671 (1992).
- ²¹L. Bengtsson, *Phys. Rev. B* **59**, 12 301 (1999).
- ²²T. Valla, P. Pervan, and M. Milun, *Appl. Surf. Sci.* **89**, 375 (1995).
- ²³C. Kittel, *Introduction to Solid State Physics*, 7th ed. (John Wiley and Sons, New York, 1996).
- ²⁴W. Bergmayer, R. Koller, C. Konvicka, M. Schmid, G. Kresse, J. Redinger, P. Varga, and R. Podloucky, *Surf. Sci.* **97**, 294 (2002).
- ²⁵C. Konvicka, A. Hammerschmid, M. Schmid, and P. Varga, *Surf. Sci.* **496**, 209 (2002).
- ²⁶H. Wormeester, M. E. Keine, E. Hüger, and E. Bauer, *Surf. Sci.* **377**, 988 (1997).
- ²⁷H. Wormeester, E. Hüger, and E. Bauer, *Phys. Rev. Lett.* **77**, 1540 (1996).